Environmental Research 215 (2022) 114371

Contents lists available at ScienceDirect

Environmental Research

journal homepage: www.elsevier.com/locate/envres

Effects of short-term hyposalinity stress on four commercially important bivalves: A proteomic perspective

S. Blanco [a,*], P. Morán [a], A.P. Diz [a], C. Olabarria [b], E. Vázquez [b]

[a] CIM – Centro de Investigación Mariña and Departamento de Bioquímica, Xenética e Inmunoloxía, Facultade de Bioloxía, Universidade de Vigo, 36310, Vigo, Spain
[b] CIM – Centro de Investigación Mariña and Departamento de Ecoloxía e Bioloxía Animal, Facultade de Ciencias do Mar, Universidade de Vigo, 36310, Vigo, Spain

ARTICLE INFO

Keywords:
Clam
Cockle
Proteome
Hyposalinity stress
Biomarker

ABSTRACT

Increased heavy rainfall can reduce salinity to values close to 0 in estuaries. Lethal and sublethal physiological and behavioural effects of decreases in salinity below ten have already been found to occur in the commercially important clam species *Venerupis corrugata*, *Ruditapes decussatus* and *R. philippinarum* and the cockle *Cerastoderma edule*, which generate an income of ~74 million euros annually in Galicia (NW Spain). However, studies of the molecular response to hyposaline stress in bivalves are scarce. This 'shotgun' proteomics study evaluates changes in mantle-edge proteins subjected to short-term hyposaline episodes in two different months (March and May) during the gametogenic cycle. We found evidence that the mantle-edge proteome was more responsive to sampling time than to hyposalinity, strongly suggesting that reproductive stages condition the stress response. However, hyposalinity modulated proteome profiles in *V. corrugata* and *C. edule* in both months and *R. philippinarum* in May, involving proteins implicated in protein folding, redox homeostasis, detoxification, cytoskeleton modulation and the regulation of apoptotic, autophagic and lipid degradation pathways. However, proteins that are essential for an optimal osmotic stress response but which are highly energy demanding, such as chaperones, osmoprotectants and DNA repair factors, were found in small relative abundances. In both months in *R. decussatus* and in March in *R. philippinarum*, almost no differences between treatments were detected. Concordant trends in the relative abundance of stress response candidate proteins were also obtained in *V. corrugata* and *C. edule* in the different months, but not in *Ruditapes* spp., strongly suggesting that the osmotic stress response in bivalves is complex and possibly influenced by a combination of controlled (sampling time) and uncontrolled variables. In this paper, we report potential molecular targets for studying the response to osmotic stress, especially in the most osmosensitive native species *C. edule* and *V. corrugata*, and suggest factors to consider when searching for biomarkers of hyposaline stress in bivalves.

1. Introduction

Changes in salinity can affect aquatic invertebrates (Hauton, 2016), especially in estuaries where strong salinity fluctuations often occur (Grilo et al., 2011; Harley et al., 2006). Estuaries are amongst the most productive types of habitat and support important fisheries (Field et al., 1998). In Galicia (NW Spain), intertidal and shallow subtidal areas support fisheries of the native clams *Ruditapes decussatus* (Linnaeus, 1758) (grooved carpet shell) and *Venerupis corrugata* (Gmelin, 1791) (pullet carpet shell), the introduced species *R. philippinarum* (Adams and Reeve, 1850) (Manila clam) and the cockle *Cerastoderma edule* (Linnaeus 1758), which together provide an income of ~74 million € a year for ~7100 fishers (http://www.pescadegalicia.gal). However, these fishing beds suffer from acute changes in salinity, such as those produced by strong precipitation events (e.g. Des et al., 2021; Parada et al., 2012; Viceto et al., 2019). During these events the river flow increases considerably, leading to a rise in the inflow of fresh water in the fishing beds and resulting in critical ecological changes and financial losses.

Although the aforementioned bivalves are euryhaline, extreme salinity fluctuations can provoke mass mortalities such as those recorded when salinity falls below 10 (Carregosa et al., 2014; Juanes et al., 2012; Parada et al., 2012; Parada and Molares, 2008; Verdelhos et al., 2015). Short-term fluctuations in salinity can also cause important sublethal effects: early recruits of *C. edule* display significantly reduced activity, i.e. continuous valve closure and inhibition of respiration and ammonium excretion rates, after two days of exposure to salinity levels below 15

* Corresponding author.
E-mail address: sofia.blanco.gonzalez@uvigo.es (S. Blanco).

https://doi.org/10.1016/j.envres.2022.114371
Received 17 June 2022; Received in revised form 29 August 2022; Accepted 15 September 2022
Available online 24 September 2022

(Peteiro et al., 2018). Adult specimens of *C. edule*, *R. decussatus*, *R. philippinarum* and *V. corrugata* exhibit a dramatic reduction in pumping activity, scope for growth (SFG) and burrowing activity after six days of exposure to salinity levels below 15 (Domínguez et al., 2020). Furthermore, reproduction is negatively affected, although the response is species-specific and varies with the gametogenic cycle (Vázquez et al., 2021).

Like other bivalves, clams and cockles are osmoconformers, i.e. their body fluid osmolarity matches that of the external environment. Thus, they can only control their osmolarity at the cellular level and/or by behavioural changes. For instance, to prevent osmotic stress, clams close their valves at salinity levels of 15 and below, and cockles do the same at salinity lower than 10 (Carregosa et al., 2014; Domínguez et al., 2020; Verdelhos et al., 2015; Woodin et al., 2020). Consequently, the SFG of the species is reduced by more than 20% of the original value, mainly due to reduced feeding activity (Domínguez et al., 2020).

At the cellular level, osmoregulation requires high energy demands, thus affecting bivalve physiology (Brett, 1979). Physiological defence mechanisms, such as heat shock proteins, free amino acid reserves and antioxidant pathways, essential for survival under stress, are energetically demanding (Eymann et al., 2020; Pörtner and Farrell, 2008; Pourmozaffar et al., 2020) and limit the energy available for growth, storage and reproduction (Kooijman and Kooijman, 2010; Petes et al., 2008; Stumpp et al., 2012; Vázquez et al., 2021). Reproductive strategies involving high energy consumption and low gonadal resorption capacity in some bivalves will hinder the optimal stress response by affecting the synthesis of energy-demanding proteins.

Although the effects of salinity stress on physiology, reproduction and behaviour (see above) have been documented in bivalves, studies of molecular responses to abiotic stressors resulting from climate change are relatively scarce. The effects of low salinity have been assessed in proteomics studies of the osmotic stress response in *Littorina saxatilis* and *L. obtusata* (Muraeva et al., 2017), detecting enzymes associated with energy metabolism and antioxidant response, chaperones, extracellular matrix and cytoskeletal proteins, ion channels, cell growth regulators and proteins potentially involved in acclimatisation to low salinity. Furthermore, chaperones and proteins involved in cytoskeleton regulation, vesicular trafficking, energy metabolism and rate of production of reactive oxygen species (ROS) have been detected in different species of the genus *Mytilus* spp. and considered candidates for involvement in the response to hyposaline stress (Tomanek et al., 2012). In *Crassostrea gigas*, gene expression related to osmoregulation, anti-apoptotic reactions, immune response, cell adhesion, cytoskeleton remodelling and cell cycling has been detected under hyposaline conditions (Zhao et al., 2012). In addition, free amino acid metabolic pathways have been described as the most important effectors for euryhaline acclimatisation in oysters (Meng et al., 2013).

The present study aimed to experimentally evaluate changes in protein abundance under short-term episodes of low salinity in the aforementioned commercially important bivalve species. The mantle edge has been reported to display higher Na^+, K^+-ATPase (NKA) activity in the clam *Rangia cunetat* and the mussel *Mytilus galloprovincialis* and to play an essential role in response to changes in environmental salinity, and it was therefore chosen as a target tissue for study (Lin et al., 2016). In addition, as gametogenesis is an energy-demanding process leading to changes in osmotic vulnerability, possible gonadal development-dependent responses (Joaquim et al., 2011; Vázquez et al., 2021) were studied by conducting experiments at two different times in the gametogenic cycle of these species (March and May).

2. Material and methods

2.1. Experimental set-up

Two low salinity stress experiments were run independently, in March and May 2016, in a mesocosm system located in a controlled temperature room (18 °C) at the Mariñas de Toralla Marine Station (ECIMAT, www.cim.uvigo.gal) belonging to the Universidade de Vigo (Galicia, NW Spain). In the mesocosm system, timer-controlled double-bellow pumps (Iwaki DP80-30) mixed dechlorinated fresh water and 50 μm-filtered seawater at ambient temperature for automatic simulation of natural tides and salinity variations. Holes (diameter, 2 cm) were drilled on the bottom of 16 L plastic tanks and were covered with 80 μm mesh (to allow water flux during low tide conditions). Four such tanks were placed inside each of four 480 L tanks (height, 50 cm x width, 80 cm x length, 120 cm) (Figs. S1A and S1B). Each 16 L tank was filled with sediment (median grain size, 0.19 mm) collected from an intertidal shellfish bed (42°11.68′ N; 8° 47.81’ W). Running 50 μm-filtered seawater entered the 480 L tanks via inlets in the bottom and exited via 30 cm tall standpipes, allowing the 16 L tanks to be completely immersed during high tide.

Adult specimens of *R. decussatus*, *R. philippinarum* and *V. corrugata* of standardised length ca. 40 mm (to minimise size-related bias) were manually collected from shellfish beds in Cambados (42°30′55″N; 08°48′53″W); specimens of the cockle *C. edule* (of standardised length ca. 30 mm) were also collected manually from shellfish beds in Noia (42°47′0″N; 8°53′0″W). The bivalves were transported to the laboratory in refrigerated coolers. Both shellfish beds located at the Rias Baixas are characterized by temperate and humid weather influenced by the upwelling regime (Méndez and Vilas, 2005) and river discharges, because of their location at shallow depths in the inner part of the rías (Alvarez et al., 2005). During rainfall events, salinity in the areas can remain at around 10 for prolonged periods and can even reach values close to 0, which persist for several days (Parada et al., 2012).

Once in the laboratory, bivalves were immediately immersed in acclimatisation tanks for 24 h. A total of 24 individuals of each species were marked and placed in different 16 L tanks (six of each species per tank) at approximately the same densities as in the shellfish beds (220 ind. m^{-2}).

Treatment consisted of a gradual reduction in salinity from 20 to 5 (treatment S5) during the 4.5 h of flood tide followed by a 1.5 h of low tide, after which salinity increased from 5 to 20 during the ebb tide (Figs. S1C and S1D). The control consisted of constant salinity of 30 (control S30) during all tidal cycles. The salinity profiles are similar to those experienced by bivalves in the field (Domínguez et al., 2020; Vázquez et al., 2021). Each salinity ramp was desynchronised by 1.5 h, the time taken to process the bivalves so that all animals remained under low tide conditions for the same length of time. Salinity stress was applied on six consecutive days. Water salinity and temperature were recorded by mini-CTDs (Star Oddi) placed inside the 480 L tanks (two tanks per salinity treatment). Salinity was measured as electrical conductivity and is therefore dimensionless.

The bivalves were fed in the evenings during the experiment with a mixture of the microalgae *Isochrysis galbana*, *Tetraselmis suecica*, *Chaetoceros gracilis* and *Rhodomonas lens*. The diet (1%) was based on the dry weight of the clams (a dry weight of 0.88 g was assumed for each individual based on the mean size).

2.2. Tissue processing

After exposure to stress conditions for six days, five individuals of each species were dug up from treatment and control tanks, washed with seawater and immediately opened by separating both valves. For proteomic analysis, a piece of mantle edge tissue of approximately 2 cm length was cut from each animal and placed in 4 mL cryovials previously cooled in dry ice and immersed in liquid nitrogen for 6 h. The cryovials were then stored in a freezer at -80 °C until processing.

To determine the gonadal stage of the specimens, a piece of tissue of ca. 1 cm^{-2} was dissected from the foot (gonad is a diffuse tissue in bivalves) and routinely processed for histology: i.e. fixed in Davidson’s fixative for 24 h, rinsed with running water for 15 min, dehydrated in an ethanol series (automatic tissue processor Leica TP1020), embedded in

paraffin (Paraffin embedding station Leica EG1150H), sectioned at 5 μm (rotary microtome Leica RM2255) and stained with haematoxylin and eosin (multistainer Leica ST5020).

The slides were examined under a microscope. Each specimen was assigned to a stage representing gonadal development, i.e. sexual rest, early gametogenesis, late gametogenesis, ripe, spawning and resorption (see Vázquez et al. (2021) for a detailed description of each category). When more than one developmental stage was observed within a single individual, a decision about the assignment of the stage was based on the condition of the majority of the follicles. The stages of gonad development were scored according to Delgado and Pérez-Camacho (2005) for *R. decussatus*, Holland (1974) for *R. philippinarum*, Cerviño Otero (2012) and Joaquim et al. (2011) for *V. corrugata*, and Martínez-Castro and Vázquez (2012) for *C. edule*.

2.3. Protein extraction, purification and trypsin digestion

Eighty individuals (twenty of each species, five per month and salinity treatment) were selected for proteomic analysis including almost equal proportions of sexes from the two experiments under the two different salinity treatments (see further details in File S1, sheet "Sample_selection"). The mantle edge from each individual was homogenised by ultrasonication in lysis buffer (7 M Urea, 2 M Thiourea and 4% CHAPS) and total protein was quantified using the Bradford method adapted to microplate format (Sánchez-Marín et al. 2021). Extractions were adjusted to a final concentration of 0.5 μg/μl in LC-MS/MS water. Proteins were purified by the acetone precipitation method, reduced by tris(2-carboxyethyl) phosphine (TCEP), alkylated by iodoacetamide (IAA) and digested with trypsin, following the protocol described by Diz and Sánchez-Marín (2021).

2.4. Isobaric labelling, multiplexing and peptide fractionation

Tryptic peptides were tagged with different isobaric tandem mass tags (TMT) from the TMT10plex™ kit (Thermo Fisher Scientific, Waltham, MA, USA) following the manufacturer's instructions. Labels were distributed among samples as indicated in File S1, sheet "Experimental_Design". Eight different TMT10plex experiments were performed for analysis of the complete set of eighty samples (see above) as each TMT10plex included ten multiplexed tagged peptide samples. Samples were randomised by species, sex and salinity treatments to minimise bias caused by run-to-run and inter-TMT10plex experiments variation. After peptide labelling, each set of ten multiplexed samples was desalted and pre-fractioned to increase the resolution of quantitative proteomic analysis with the Pierce High pH Reversed-Phase Peptide Fractionation Kit (Thermo Fisher Scientific), thus producing eight fractions with peptides separated according to their polarity. Peptides were dried in a Vacuum Concentrator (Eppendorf™ Vacufugue™ Concentrator).

2.5. LC-MS/MS analysis

Dried peptides from each fraction were resuspended in 0.5% formic acid for tandem mass spectrometry analysis (MS/MS) carried out in a Thermo LTQ-Orbitrap Elite device coupled to a Proxeon EASY-nLC II liquid chromatography system (Thermo Fisher Scientific) operated in a higher-energy collisional dissociation (HCD) mode. The analysis followed the parameters described by Mateos et al. (2019).

2.6. Protein identification and quantification

Protein identification and quantification were performed with PEAKS® X Pro software (Bioinformatics Solutions Inc., Waterloo, Canada). All MS and MS/MS spectra were compared to a consensus protein database constructed after combining all available RNA sequences (TSA database, March 22) translated into the six reading frames for *R. philippinarum* (Bioprojects PRJNA137531, PRJNA426752, PRJNA298283 and PRJNA672267 including 5,129,558 sequences from all tissues) and *R. decussatus* (236,989 sequences from the project PRJNA170474, which includes gonadal tissues from 12 females and 12 males), the translated proteins (14,134 sequences) from gene predictions (Holt and Yandell, 2011) of the *C. edule* genome (Bruzos et al., unpublished) and 27 protein sequences available in NCBI for *V. corrugata*. Despite the significantly lower number of sequences representative of *V. corrugata*, the decompensation in the database did not affect the capacity to detect differences between salinity treatments for this species (see Table 1) as the identifications were made against sequences of the other species. Sequence redundancy was removed using the CD-HIT software with a similarity threshold of 0.9. This customised database also included a list of sequences from contaminants commonly found in proteomic analysis (cRAP) and decoy sequences to calculate the false discovery rate (FDR). The mass tolerance for precursor and fragment ions was set at 10 ppm and 0.02 Da, respectively, allowing a maximum of two missed cleavages for the identification. Carbamidomethylation at cysteine residues and TMT10plex were marked as fixed modifications, while oxidation at methionine and N-terminal acetylation were considered variable modifications. More than two matching peptide sequences and at least one unique peptide were required parameters for protein identification. For reporter ion-based quantification, unique peptides with a score higher than FDR $\leq$5% and a quality $\leq$8 were considered.

2.7. Differential abundance analysis

Intra- and inter-experimental CONSTANd-inspired (Van Houtven et al., 2021) normalisation of relative protein abundance was performed following the procedure explained in Diz and Sánchez-Marín (2021) and successfully applied by Sánchez-Marín et al. (2021). Normalised data were log2 transformed to meet the assumptions of normality and homoscedasticity required in parametric statistics.

To determine whether there were any significant variations in the mantle-edge proteome between months, salinity treatments and the interaction between both factors, two-way ANOVAs (RStudio Team, 2020) were performed for each species. The p-values obtained were adjusted to reduce the false discovery rate (FDR) derived from multiple testing by applying the SFisher correction method (see Diz et al., 2011) of the SGoF + v.3.8 software (Carvajal-Rodriguez and Uña-Alvarez, 2011).

Analysis of differential abundance of proteins between salinity treatments was performed for species and month by applying a Student's t-test to each protein. A minimum set of three individuals per salinity treatment was required, and zeros (abundance values not reaching the minimum detection threshold) were considered the minimum value of the variable within the control/treatment group. The p-values obtained were adjusted and differentially abundant proteins for a q-value < 0.05 (Storey, 2003) were discussed.

For differentially abundant proteins ($q < 0.05$), enrichment analyses (Fisher's test) of GoTerms and KEGG pathways were performed to test their potential relationship with the osmotic stress response. Enrichment results were represented with bar charts showing the percentage of sequences the GoTerms or KEGG suppose in the test set ($q < 0.05$) versus the percentage they represent in the reference set with the total number of sequences quantified for that species and month. Conserved domain analyses were performed with InterProScan (Blum et al., 2021) for differentially abundant proteins ($q < 0.05$) and to explore differentially quantitative profiles in all quantified chaperone-domain proteins.

Heat maps were constructed with ClustVis (Metsalu and Vilo, 2015) using Ward's method for hierarchical clustering based on Euclidean distance estimation. PCAs were performed with RStudio (RStudio Team, 2020) using the singular value decomposition.

Table 1
Proteins with significantly differential abundance (q-value < 0.05) between salinity treatments for the different species and months with potential involvement in response to osmotic stress. Only the aquaporin AQPAe.a-like shows a slightly higher significance level (q-value = 0.07). Those proteins without informative description and whose estimated function is based on the analysis of conserved domains are tagged with an (*).

Species	Month	Protein description	Function	Fold Change (S5/S30)
V. corrugata	**March**	aquaporin AQPAe.a-like	osmoregulation	11.44
		hypothetical protein DPMN_055454	ROS detoxification (*)	1.53
		NADH: quinone oxidoreductase isoform X3	ROS production	1.45
		elongation factor Tu	autophagy	1.44
		Rho-type guanine nucleotide exchange factor 11 isoform X32	cytoskeleton stabilisation	1.30
		stress response protein PHOS34	stress response	0.86
		UDP glucose 4-epimerase	osmoprotectant	0.64
		granulins-like isoform X4	ER-stress response	0.020
		C-Jun-amino-terminal kinase-interacting protein 4-like isoform X3	DNA repair/apoptosis	absence in S5
		solute carrier family 2 facilitated glucose transporter member 1-like isoform X1	osmoregulation	absence in S5
		lactoylglutathione lyase-like	ROS detoxification	absence in S5
	May	nicotinamide phosphoribosyltransferase-like	DNA repair	absence in S30
		unc-87 Calponin homolog OV9M	actin remodelling	absence in S30
		actophorin-like protein	actin remodelling	9.19
		hypothetical protein DPMN_055454	ROS detoxification (*)	4.53
		semaphorin-5B-like	autophagy	0.56
		serine/threonine-protein phosphatase 2 A catalytic subunit beta isoform	ER-stress response/mitophagy	0.26
		vacuolar protein sorting-associated protein 33 A-like isoform X2	autophagy	absence in S5
C. edule	**March**	dual oxidase 2-like isoform X1	ROS production/phagocytosis	absence in S30
		excitatory amino acid transporter-like	aminoacid transport	absence in S30
		unconventional myosin-XVIIIa-like isoform X3	vesicular traffic	4.71
		Ras-related protein Ral-a	apoptosis	4.41
		acyl-CoA-binding protein-like	beta-oxidation	3.28
		Cu/Zn-superoxide dismutase	ROS detoxification	2.04
		T-complex protein 1 subunit epsilon	chaperone	1.84
		vacuolar protein sorting-associated protein 13 A-like isoform X3	autophagy	0.77
		NADH:quinone oxidoreductase subunit B2-like	ROS production	0.45
		heat shock protein 20	chaperone	0.43
		actophorin-like protein	actin-binding	0.43
		NADH dehydrogenase [ubiquinone] 1 alpha subcomplex subunit 2-like	NAD^+ shynthesis	0.21
		collagen type XVIII alpha	EM structural constituent	0.10
		prohibitin 2	chaperone	0.0083
	May	heparanase	EM remodelling	absence in S30
		NipSnap-like protein isoform X2	Ca^{2+} channel activity/mitophagy	absence in S30
		Titin	Ca^{2+} and calmodulin-binding	3.52
		disulphide isomerase	chaperone	3.40
		nicotinamide phosphoribosyltransferase-like	NAD^+ synthesis	1.66
		phosphatidylinositol-binding clathrin assembly protein	membrane curvature regulation	1.53
		semaphorin-5B-like	apoptosis	1.39
		prohibitin 2	chaperone	0.95
		hypothetical protein DPMN_055454	ROS detoxification (*)	0.52
		dynein light chain roadblock-type 2 isoform X1	microtubule-binding	0.17
		aldehyde dehydrogenase mitochondrial-like	detoxification	0.15
		ras-related protein Rab-5B-like	apoptosis	0.13
		NADH dehydrogenase [ubiquinone] 1 alpha subcomplex subunit 8	NAD^+ shynthesis	absence in S5
R. decussatus	**March**	choline transporter-like protein 2 isoform X3 involved	membrane synthesis	absence in S30
		band 7 protein AGAP004871-like isoform X3	transmembrane cation transport	0.41
	May	tubulin alpha-1A chain	cytoskeleton organisation	absence in S30
		tubulin beta-4B chain	cytoskeleton organisation	absence in S5
R. philippinarum	**March**	dolichyl-diphosphooligosaccharide-protein glycosyltransferase	ER-stress response	absence in S30
		plectin-like isoform X4	osmoprotectant	1.61
	May	vacuolar protein sorting-associated protein 33 A-like isoform X2	autophagy	absence in S30
		nicotinamide phosphoribosyltransferase-like	NAD^+ synthesis	absence in S30
		dihydrolipoyllysine-residue acetyltransferase	lipid metabolism	1.33
		T-complex protein 1 beta-like subunit	chaperone	0.54
		manganese superoxide dismutase	detoxification	0.45
		ATP-dependent RNA helicase DDX3X	oxidative stress response	0.25
		ubiquinone biosynthesis monooxygenase COQ6 mitochondrial-like	ROS-production	0.18
		NA	protease inhibitor (*)	0.032
		filamin-A-like isoform X1	osmoprotectant	0.022

3. Results

3.1. Gonadal development stages and month-dependent variations in the mantle-edge proteome

Histological analysis revealed variations in gonadal developmental stages between species, months and salinity treatments (Fig. 1) (for further details on histological analysis, see Vázquez et al., 2021). Except for *R. decussatus*, all species were mature, spawning or showed gonadal resorption. *R. decussatus* had abnormal gonads with enlarged nuclei in the oocytes, while *R. philippinarum* showed increased gonadal resorption under hyposaline conditions, as occurs under normal conditions. In March, *C. edule* and *V. corrugata* displayed a mass spawning strategy under stress, the latter showing some capacity for gonadal resorption.

Significant changes were also observed between mantle-edge protein profiles for *V. corrugata* and *R. philippinarum*, with 69.46% and 60.93% significantly differentially abundant proteins (2-way pooled ANOVA, SFisher < 0.05) between months. In *C. edule* and *R. decussatus*, the

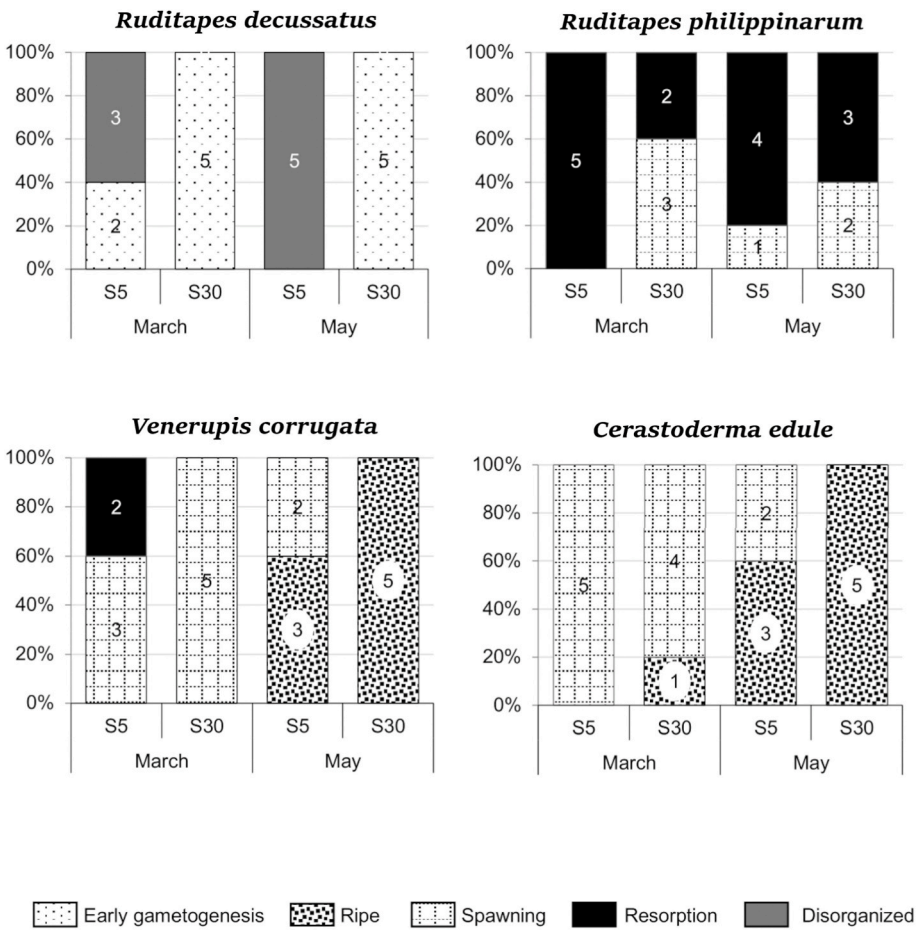

Fig. 1. Gonadal development stages of the different species in months and salinity treatments (S30: control, S5: hyposalinity treatment). All species except *R. decussatus* were at gonadal maturity, spawning or gonadal resorption. In *R. decussatus*, individuals with abnormal gonads and enlarged nuclei oocytes were observed under hyposaline conditions. *R. philippinarum* showed increased gonadal absorption with haemocyte infiltration, a phenomenon also observed under normal conditions, while *C. edule* and *V. corrugata* exhibited a stress response involving mass spawning and some gonadal resorption in the case of *V. corrugata* in March.

variation was smaller, accounting for 12.81% and 12.50% of differentially abundant proteins. PCAs show the levels of variation between months for the different species (Fig. 2). No interaction between the two factors was detected and there were no differences between salinity treatments when months were combined (Sfisher = 1), even for those species where the "month" factor was slightly discriminant. These results justify the study of variations between salinity treatments by species and months.

3.2. Variations in protein abundance levels between salinity treatments

After removing proteins with fewer than three samples per salinity treatment, between 2424 and 2807 proteins were quantified in the four species (see File S1, sheet "proteins_differential_abundance" for more details), with a significantly greater number of proteins quantified in May (binomial exact test, $p < 0.05$) than in March in all cases. The volcano plots (Fig. 3) showed that *C. edule* in March had the largest number of differentially abundant proteins ($p < 0.05$) relative to all other species and months, with 299 and 69 proteins being significantly more abundant in S5 and S30 respectively. *C edule* was the species with the largest number of differentially abundant proteins between salinity treatments in both months after the multiple testing correction ($q < 0.05$), followed by *V. corrugata*, *R. philippinarum* and *R. decussatus*. In addition, the difference increased significantly to 118 in cockles *C. edule* in March when the q-value threshold was augmented to 0.1 (Fig. 4a). This was the only case in which the PCA (Fig. 4b) and the heat map (Fig. 4c) showed clustering of samples by salinity treatment, suggesting modulation of protein abundance profiles influenced by hypoosmotic conditions.

The analysis of conserved domains (File S1, sheet "InterPro_conserved_domains") for differentially abundant proteins ($q < 0.05$) (Fig. 4d) showed a high frequency of proteins with transmembrane, ion/RNA/cytoskeleton-binding domains; as well as oxidoreductases, chaperones, involved in vesicular transport, mitochondrial and extracellular matrix proteins.

File S1 ("proteins_differential_abundance" sheet) lists all proteins that differed in abundance between salinity treatments for the different species and months, together with their significance level (p-value and q-value) and effect size (fold change, presence/absence).

3.2.1. Enrichment analysis

Enrichment analyses (Fisher's test, $p < 0.05$) of GoTerms (Figs. S2A and B) and KEGG pathways (Figs. S3A and B) were performed for those species and months with the largest number of differentially abundant proteins. Analyses were performed independently for those proteins that were significantly more abundant (Figs. S2A and S3A) and less abundant (Figs. S2B and S3B) in S5 conditions relative to controls, with a maximum of thirty enriched terms.

3.2.1.1. Venerupis corrugata. In March, GoTerms modulating NADPH/$NADP^+$ redox homeostasis through the pentose phosphate pathway were detected in large relative abundances under hypoosmotic conditions. The overrepresented KEGG pathways were mainly involved in lipid metabolism and actin cytoskeleton regulation. Transmembrane transport, disulphide oxidoreductase activity, mitochondrial organisation and micronutrient uptake pathways were detected in low abundances. In May, lipid metabolism and pyridine nucleotide biosynthesis involved in regulating intracellular Ca^{2+} and redox homeostasis (Kilfoil et al., 2013) were present in greater abundances under stress conditions. By contrast, protein depolymerisation, cell organisation and disulphide

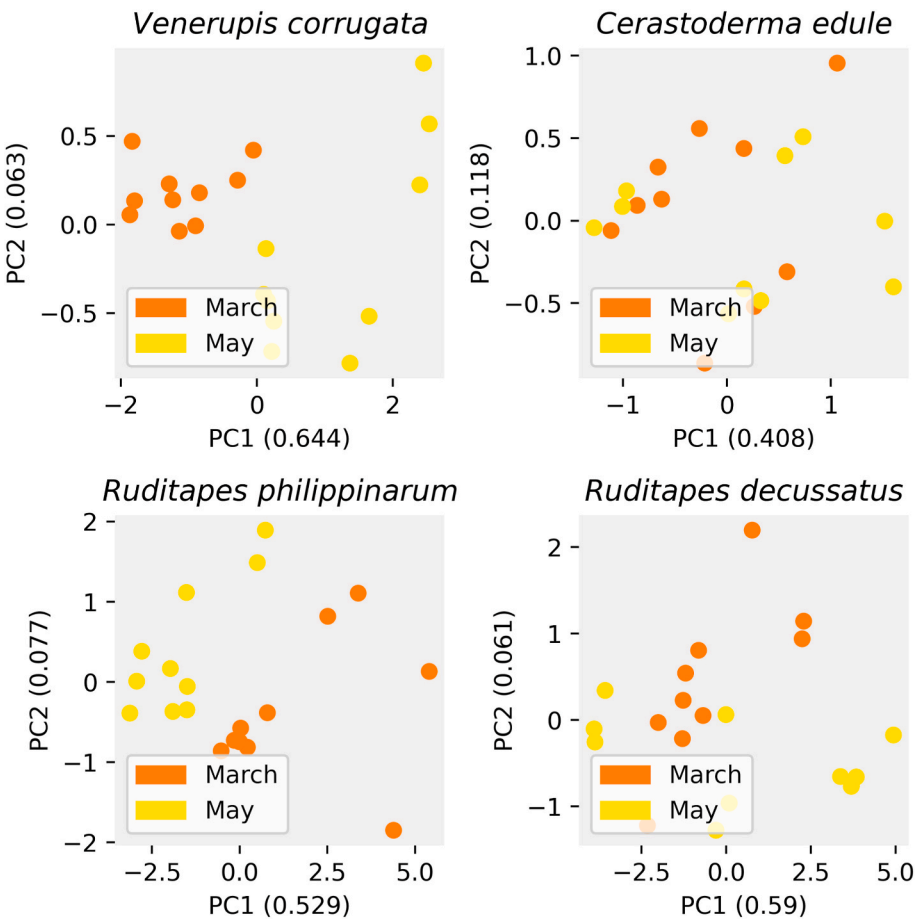

Fig. 2. PCAs of the different species by month as a discriminatory factor. In *V. corrugata* and *R. philippinarum*, the species with the largest number of differentially abundant proteins (2-way ANOVA, SFisher $<$ 0.05) between months (69.46% and 60.93%, respectively), clear clustering of individuals by sampling time point was observed. In *C. edule* and *R. decussatus*, with 12.81% and 12.50% of differentially expressed proteins respectively, there was no clustering. However, there were no differences between salinity treatments when combining months in any of the cases, even for those species where there was no clustering by sampling time.

reductase activity were detected in lower abundances. KEGG pathways of apoptosis, meiosis and regulation of pluripotency were also found in lower abundances.

3.2.1.2. Cerastoderma edule. In March, stress response functions, antioxidants, proteins involved in detoxification and nucleotide and cation binding, among others, were detected in greater abundance in hyposaline conditions. Mitophagy, apoptosis and p53-mediated signalling (activated by stress caused by DNA damage and ROS) KEGG pathways also were found to increase. Functional proteins involved in cation binding and actin organisation and also cytoskeleton, organelles and mitochondrial cellular components were detected in low abundances. In May, increased nucleotide biosynthetic activity, oxidoreductase functions and NAD^+ homeostasis pathways were detected. Dehydrogenases, nucleases, gene silencing, the pentose phosphate pathway and the DNA repair activity were detected in low abundance under stress conditions.

3.2.1.3. Ruditapes philippinarum. In May, functional proteins related to metabolism and biosynthesis of nitrogen and phosphorus compounds, autophagy and oxidoreductase activity appeared in greater abundance under hyposaline conditions. Oxidative, stress-response and cation binding functional proteins were detected in low abundance. KEGG pathways involving ubiquinones and the transcription factor forkhead box O (FOXO), which transactivates genes involved in oxidative stress resistance, energy metabolism, DNA damage repair and protein chaperone protection (Storz, 2011), were also detected in low abundance.

3.2.2. Proteins potentially involved in the osmotic stress response

This section reports differentially abundant proteins ($q < 0.05$) between salinity treatments and potentially involved in response to osmotic stress. The list of proteins, including their functional category and effect size, is summarised in Table 1.

To close the section, trends in relative abundance patterns of proteins between months were analysed for those significantly differential abundant proteins between salinity treatments ($q < 0.05$) in at least one month. Table 2 lists those proteins with matching trends (FC greater or lower than one in March and May) at both sampling times (see File S1, "fold_changes_trend" sheet).

3.2.2.1. Venerupis corrugata. In March, the ROS-producing NADH: quinone oxidoreductase (Vinogradov and Grivennikova, 2016) was detected in greater abundance under osmotic stress. Translation factors with an autophagic function were also detected, including the elongation factor Tu (Lei et al., 2012) and the Rho-type guanine nucleotide exchange that stabilise the cytoskeleton and osmorregulates (Di Ciano-Oliveira et al., 2006; Kino et al., 2010). The aquaporin AQPAe. a-like was also detected when the significance threshold was increased to $q < 0.1$. The universal stress response protein PHOS34 and the UDP glucose 4-epimerase involved in the synthesis of the osmoprotectant trehalose (Tang et al., 2018) were detected in lower abundances under hypoosmotic stress. The granulins-like isoform X4, whose precursor mediates endoplasmic reticulum (ER) stress caused by unfolded proteins (Li et al., 2014), was also detected. The C-Jun-amino-terminal kinase-interacting protein 4-like isoform X3, which mediates apoptotic and DNA repair pathways (Johnson and Nakamura, 2007), the osmoregulator solute carrier family 2 facilitated glucose transporter member 1-like isoform X1 and the lactoylglutathione lyase-like, specifically involved in the detoxification of reactive species (Cianfruglia et al., 2020) were only detected in controls. In May, the nicotinamide phosphoribosyltransferase-like protein involved in NAD^+ synthesis,

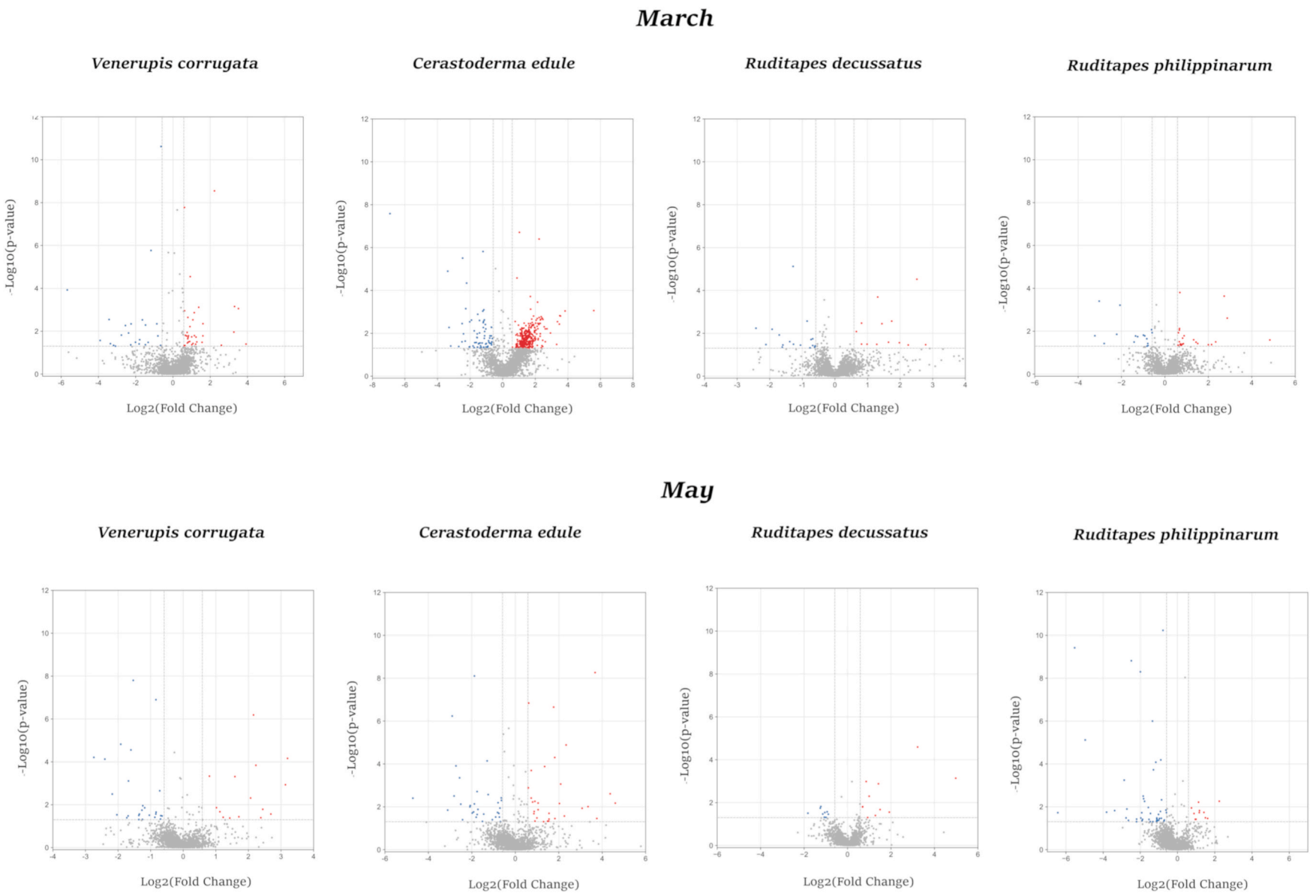

Fig. 3. Volcano plots with all proteins quantified for the different species and months. The proteins present at significantly lower abundances ($p < 0.05$) in the hyposaline treatment than the control are highlighted in blue, with higher abundances indicated in red and those with no significant change in abundance indicated in grey. In *C. edule* in March, the largest number of differentially abundant proteins was observed: 299 with greater abundance in S5 and 69 in S30. (For interpretation of the references to colour in this figure legend, the reader is referred to the Web version of this article.)

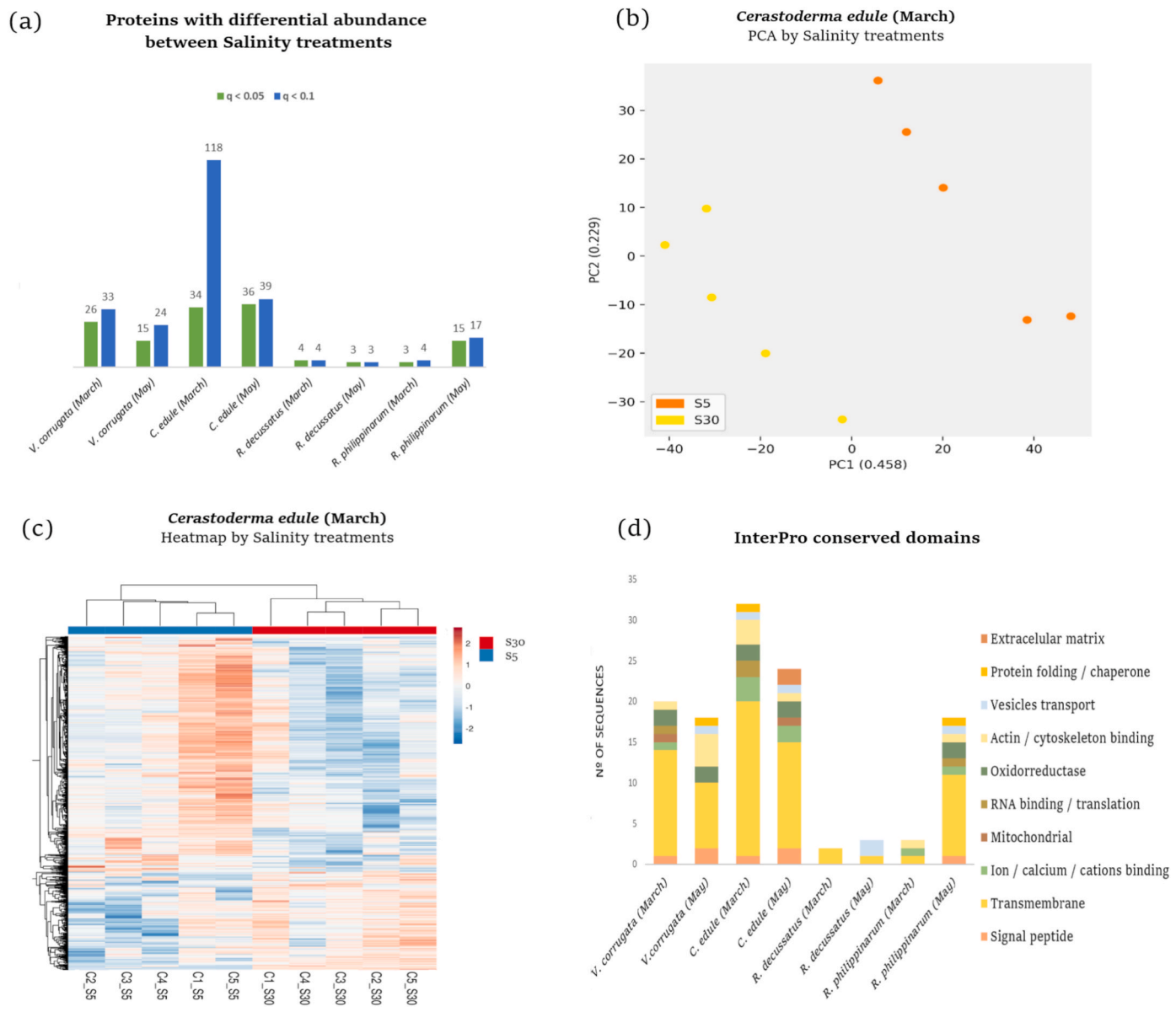

Fig. 4. (a) Differentially abundant proteins detected between salinity treatments considering significance thresholds of $q < 0.05$ (green) and $q < 0.1$ (blue). In March, only *C. edule* showed a significant increase in differentially abundant proteins when the threshold was increased to $q < 0.1$. (b) PCA and (c) heat map with all proteins quantified in March in *C. edule*, showing clustering by salinity treatment in both cases. (d) Result of the analysis of conserved domains for differentially abundant proteins ($q < 0.05$). Categories were based on the most abundant domains with potential involvement in the response to osmotic stress and are not exclusive (a protein may contain more than one domain). (For interpretation of the references to colour in this figure legend, the reader is referred to the Web version of this article.)

which plays a key role in DNA repair, resistance to oxidative stress and cell death (Massudi et al., 2012), together with the actin remodelling protein unc-87 Calponin homolog OV9M, were detected only under stress conditions. The actophorin-like protein, which is involved in actin depolymerisation, was detected at significantly increased abundance in S5 individuals. The serine/threonine-protein phosphatase 2 A catalytic subunit beta isoform that takes part in ER stress signalling pathways, mitophagy and the cellular response to Ca^{2+} ions (País et al., 2009) and the semaphorin-5B-like with immune response and autophagy function, were detected in low abundances. The autophagy regulator vacuolar protein sorting-associated protein 33 A-like isoform X2 was absent in S5. The hypothetical protein DPMN_055454 was detected in significantly greater abundance under hyposaline conditions in both months and showed both conserved glutaredoxin and disulphide oxidoreductase domains and a 62% coverage (e value $= 2 \times 10^{-176}$) with a glutaredoxin from *Elysia marginata*, implicated in minimising oxidative cell damage.

3.2.2.2. Cerastoderma edule. In March, the dual oxidase 2-like isoform X1, which is involved in ROS production and phagocytosis, was detected only under hyposaline conditions, as was the high-affinity osmosensitive Na^{+}-dependent excitatory amino acid transporter-like. The metalloprotein Cu/Zn-superoxide dismutase, which catalyses the conversion of superoxide radical anions into O_2 and H_2O_2 (Wang et al., 2018), the chaperone T-complex protein 1 subunit epsilon, proteins involved in vesicular traffic such as the unconventional myosin-XVIIIa-like isoform X3 and the acyl-CoA-binding protein-like, involved in lipid beta-oxidation, were detected in high abundances. The apoptosis inhibitor Ras-related protein Ral-a was also detected. However, the heat shock protein 20 (HSP20) and the mitochondrial chaperone prohibitin 2 were detected in relatively low abundances. Actin-binding proteins such

Table 2
Proteins potentially involved in the response to hyposalinity with concordant abundance levels between March and May (Fold changes above or below 1 in both months).

	Description	FC (S50/S30) - March	FC (S50/S30) - May
V. corrugata	nicotinamide phosphoribosyltransferase-like	1.18	absence in S30
	unc-87 Calponin homolog OV9M	2.33	absence in S30
	aquaporin AQPAe.a-like	11.44	1.49
	hypothetical protein DPMN_055454	1.53	4.46
	rho guanine nucleotide exchange factor 11 isoform X32	1.29	1.04
	vacuolar protein sorting-associated protein 33 A-like isoform X2	0.84	absence in S5
	lactoylglutathione lyase-like	absence in S5	0.76
C. edule	Ras-related protein Ral-a	4.41	2.07
	T-complex protein 1 subunit epsilon	1.84	1.23
	phosphatidylinositol-binding clathrin assembly protein	1.32	1.53
	nicotinamide phosphoribosyltransferase-like	1.02	1.66
	vacuolar protein sorting-associated protein 13 A-like isoform X3	0.78	0.81
	hypothetical protein DPMN_055454	0.46	0.52
	actophorin-like protein	0.43	0.65
	NADH dehydrogenase [ubiquinone] 1 alpha subcomplex subunit 2-like	0.21	0.79
	prohibitin 2	0.01	0.95
	ras-related protein Rab-5B-like	abscense in S30	0.13
R. decussatus	band 7 protein AGAP004871-like isoform X3	0.41	0.79
R. philippinarum	NA	0.64	0.032

as the actophorin-like protein and extracellular matrix (EM) structural constituents like the collagen type XVIII alpha were also detected. The NADH: quinone oxidoreductase (Na^+ -NQR), the NAD^+ synthesiser NADH dehydrogenase [ubiquinone] 1 alpha subcomplex subunit 2-like and the autophagy regulator vacuolar protein sorting-associated protein 13 A-like isoform X3 were also found in low abundances. In May, heparanases involved in (EM) remodelling and proteins related to the positive regulation of Ca^{2+} channel activity and mitophagy, such as the NipSnap-like protein isoform X2, were detected only under stress conditions. The ER -chaperone protein disulphide isomerase (PDI), Ca^{2+} and calmodulin-binding proteins such as titin, NAD^+ synthesis proteins, such as the nicotinamide phosphoribosyltransferase-like and the semaphorin-5B-like, which participate in the regulation of apoptotic signalling and the immune response, were significantly more abundant. The phosphatidylinositol-binding clathrin assembly protein, which regulates membrane curvature, was also detected in high abundance. The mitochondrial dehydrogenase-like aldehyde which removes toxic aldehydes from oxidative stress (Sydow et al., 2004), the ras-related protein Rab-5B-like, a microtubule-binding component, the light chain roadblock-type 2 isoform X1 and the hypothetical protein DPMN_055454 were less abundant. The mitochondrial chaperone prohibitin 2 was slightly less abundant under stress conditions. Although absent under hyposaline conditions, the NADH dehydrogenase [ubiquinone] 1 alpha subcomplex subunit 8 was also detected.

3.2.2.3. Ruditapes decussatus. The choline transporter-like protein 2 isoform X3 involved in lipid membrane synthesis was detected only under stress conditions in March, while the 7 protein AGAP004871-like isoform X3 modulating transmembrane cation transport was present in low abundance (Stewart, 1997). In May, the tubulin alpha-1A chain was only detected in low salinity conditions, while the tubulin beta-4B chain was only detected in control salinity conditions.

3.2.2.4. Ruditapes philippinarum. The dolichyl-diphosphooligosaccharide-protein glycosyltransferase, involved in protein maturation and detection of unfolded proteins in the ER, was only detected in individuals exposed to low salinity in March. The plectin-like isoform X4, an osmoprotectant actin-binding protein (Osmanagic-Myers et al., 2015), was obtained at higher abundance under hyposaline conditions. In May, the vacuolar protein sorting-associated protein 33 A-like isoform X2 involved in autophagic pathways and the nicotinamide phosphoribosyltransferase-like that synthesises NAD^+ were only detected only under osmotically stressful conditions. The dihydrolipoylly sine-residue acetyltransferase, involved in lipid metabolism (Ballantyne and Moyes, 1987), was detected in significantly greater abundance. Proteins detected in low abundances included the mitochondrial manganese superoxide dismutase, which detoxifies free radicals (Candas and Li, 2014), the mitochondrial COQ6-like ubiquinone oxidoreductase biosynthesis monooxygenase, the T-complex chaperone protein 1 beta-like subunit, the ATP-dependent RNA helicase DDX3X involved in the response to oxidative stress (Saito et al., 2021) and cytoskeleton proteins such as the filamin-A-like isoform X1, which reduce osmotic stress-driven water flow (Ito and Yamazaki, 2006). A protein without informative annotation presenting a cystatin superfamily conserved domain was also detected in low abundance. Proteins of this superfamily were observed in greater abundance in *M. trossulus* under hyposaline stress conditions (Tomanek et al., 2012).

In *V. corrugata*, 67% (10/15) of the proteins that were differentially abundant ($q < 0.05$) between salinity treatments had concordant fold changes between March and May, more than the 50% expected by chance. Among the 10 proteins with concordant fold changes, 7 were reported as potentially involved in the response to hyposalinity in bivalves (including the aquaporin, with a $q < 0.1$). In *C. edule*, the percentage of concordance was 56% (15/20), with 10 out of the 15 matching proteins being candidates for osmotic stress response. In *R. decussatus* and *R. philippinarum*, with a smaller number of proteins with differential abundance between salinity treatments, only 25% (1/4) and 13% (1/8) of the proteins, respectively, showed concordant fold changes. In both cases, only 1 protein was concordant between months, corresponding to a protein considered potentially involved in the stress response.

3.3. Chaperone-domain proteins

Given the importance of the study of chaperones in response to osmotic stress, the abundance profiles of proteins with conserved chaperone-like domains were analysed. Only in March, *C. edule* samples were clustered by salinity treatment when considering the abundance of chaperone domain proteins, with 43 over 67 showing greater abundance under high salinity conditions (fold change >1) (Fig. S4). For that species and month, differential abundance of chaperon proteins ($q < 0.1$) was detected; the epsilon subunit of the T-complex protein (FC = 1.84) and the peptidyl prolyl *cis-trans* isomerase B (FC = 11.67), with a conserved peptidyl prolyl *cis-trans* isomerase (PPIase)-like domain which accelerates protein folding, together with the mitochondrial stress-70-like osmoprotectant protein (FC = 2.26) (Shim et al., 2002) were detected in relatively high abundances under saline stress. However, low abundances of the heat shock protein 20 (FC = 0.4) and the mitochondrial chaperone prohibitin 2 (FC = 0.008) were detected. In May, the ER chaperone protein disulphide isomerase (PDI) (FC = 3.4) was present in relatively high abundance. Chaperone domain proteins such as the isoform X of the ubiquitin carboxyl-terminal hydrolase CYLD-like (FC = 0.15), also with a PPIase domain, and the beta-like subunit of the T-complex 1 protein (FC = 0.15), were significantly less

abundant under hypoosmotic conditions in both *V. corrugata* and *R. philippinarum*, respectively.

4. Discussion

In this proteomic analysis of the mantle edge tissue from four bivalve species subjected to short-term hyposaline stress, significantly differentially abundant proteins were detected between March and May in all species, with highly divergent protein abundance profiles in *V. corrugata* and *R. philippinarum*. This indicates that the different gametogenic stages of the species, months considered and salinity treatments would cause changes in the proteomic profile of the mantle edge, strongly suggesting that reproductive stages affect the stress response. The combination of month-dependent controlled (i. e. sampling time, gonadal development stage) and uncontrolled factors would explain these differences in the proteome. Consequently, combining individuals sampled at different time points would decrease the statistical power when detecting differential abundance of proteins between salinity treatments, which supports the evidence of greater proteome-wide effects due to temporal sampling (e.g Timmins-Schiffman et al., 2017) than those related to the salinity conditions tested. This greater variation in the proteome over the months than over the treatment has also been observed in other studies (e.g. Sánchez-Marín et al. (2021).

The largest number of proteins affected by the salinity treatments were detected in *C. edule*. In March, the month when spawning events peaked (Martínez-Castro and Vázquez, 2012), an increase in ROS levels was possibly derived from an enhanced rate of oxidative metabolism in response to stress (Redza-Dutordoir and Averill-Bates, 2016). The elevated levels of ROS are related to an increased abundance of ROS scavengers such as the osmosensitive excitatory amino acid transporter (Malik and Willnow, 2019) and ROS detoxification proteins (Wang et al., 2018). These also stimulate apoptotic and autophagic pathways that recycle cellular components, compensating for the low uptake rate produced by valvar closure (Rambold and Lippincott-Schwartz, 2011). Lipid metabolism, which acts as a hypoosmotic resistance factor in oysters (Ballantyne and Moyes, 1987), may also compensate for the decrease in intake. The high levels of the T-complex chaperone protein 1 would promote actin and tubulin folding, whose polymerisation rates are altered by abiotic stress factors (Tomanek, 2012). However, chaperones with a high biosynthetic cost such as the HSP20 and prohibitin 2 were detected in low abundances (Eymann et al., 2020; Pörtner and Farrell, 2008). Cytoskeleton remodelling proteins, damaged by osmotic stress (Balbi et al., 2021), proteins with NAD^+ synthesis function, and a molecule involved in redox homeostasis and DNA repair (Alves de Almeida et al., 2007) were also found in low abundances. In May, there was an increase in proteins involved in EM remodelling and regulation of membrane curvature to balance external osmotic pressures (Lu et al., 2006), as well as ER redox-dependent chaperones that fold damage proteins after osmotic shock (Soares Moretti and Martins Laurindo, 2017). The amounts of proteins that positively regulate actin-binding channel activity in response to Ca^{2+} and calmodulin, oxidoreductases and that are involved in mitophagy processes, activated after mitochondrial damage due to oxidative stress, also increased (Steffen et al., 2020). Nevertheless, proteins involved in DNA repair pathways, oxidoreductases, the mitochondrial chaperone prohibitin 2 and cytoskeleton remodelling proteins were detected in small amounts probably because they are energetically demanding. These results are consistent with observations in *Littorina saxatilis*, *L. obtusata* (Muraeva et al., 2017) and *Crassostrea gigas* (Zhao et al., 2012) under hyposaline conditions. Modulation of energy metabolism, antioxidant response, apoptotic pathways and cytoskeletal remodelling have also been described in these species under osmotic stress. In addition, Muraeva et al. (2017) linked a larger set of altered proteins with increased sensitivity to osmotic stress, which is consistent with the detection of low abundances of several proteins essential for the stress response in *C. edule*. The concordant abundance levels of seven candidate proteins between months support their biological relevance and potential involvement in the stress response. These include the chaperones T-complex protein 1 subunit epsilon and prohibitin 2 (the first in high and the second in low abundance), as well as proteins involved in the regulation of the membrane curvature, autophagy, apoptosis, detoxification and NAD^+ synthesis. These results are consistent with the findings of previous physiological and behavioural studies (Domínguez et al., 2020) and with greater mortality at low salinity described in *C. edule* (Carregosa et al., 2014; Parada et al., 2012; Peteiro et al., 2018; Verdelhos et al., 2015).

Despite the low number of *V. corrugata* proteins in the database, this species showed a larger number of differentially abundant proteins relative to species with species-specific and whole-tissue transcriptome representation, such as *R. philippinarum*. *V. corrugata* has a low capacity to isolate from the hyposaline environment because it is unable to complete valve closure (Carregosa et al., 2014; Parada et al., 2012). In both months, the response to osmotic stress was similar to that in *C. edule*, suggesting that the greatest modulations were observed in those species in which valve closure is incomplete (Gharbi et al., 2016) and with a massive spawning reproductive strategy under low salinity stress (Vázquez et al., 2021), a stressful phenomenon that would by itself condition an adequate osmotic shock response (Petes et al., 2008). *V. corrugata* also modulated redox homeostasis, lipid metabolism, cytoskeletal remodelling and autophagic pathways. High-energy demandant proteins involved in osmoregulation and cytoprotection, including those that repair DNA and regulate the ER-stress response, reappeared at a low frequency. As in *C. edule*, in this species, ten proteins with concordant differential abundance between months were detected, including the AQPAe.a-like aquaporin in high abundance and, as in cockles, proteins involved in actin and cytoskeleton remodelling that could modulate cell volume, in autophagy, ROS detoxification and NAD^+ synthesis.

Both species of the genus *Ruditapes* spp., with complete valve closure (Gharbi et al., 2016) and reproductive strategies focused on energy saving through either delayed gonadal development (*R. decussatus*) or gonadal reabsorption (*R. philippinarum*), had fewer differentially abundant proteins between salinity treatments. The already described higher level of tolerance to low salinity in *R. decussatus* (Bidegain and Juanes, 2013; Domínguez et al., 2020; Juanes et al., 2012) was confirmed by the small number of differentially abundant proteins detected and the large abundance of osmoprotectant precursors detected in March. As a consequence, the number of proteins with consistent abundances between months was significantly lower than expected by chance. In March, the month with the highest resorption rate under hyposaline conditions in *R. philippinarum*, factors involved in the detection of ER-unfolded proteins and the stabilisation of the cytoskeleton were detected in large abundances. However, in May, the response was similar to that observed in *C. edule* and *V. corrugata*. This could explain the high mortality rate of *R. philippinarum* in natural conditions when flooding occurs during reproductive periods, higher than that described in *R. decussatus* (Bidegain and Juanes, 2013; Juanes et al., 2012).

Our findings suggest modulations in the mantle-edge proteome under osmotic stress conditions in *C. edule*, *V. corrugata* and *R. philippinarum* in May. However, energetically demanding proteins crucial for the stress response, such as antioxidants, chaperones and DNA repair factors, were detected in low abundances, which would prevent an optimal response to hyposaline conditions. Although the more stress-tolerant *R. decussatus* did not show alterations at the molecular level, *R. philippinarum* showed a high capacity for gametogenic regeneration (Delgado and Pérez-Camacho, 2007). Consequently, faster maturation, together with a larger number of spawning events observed in the Manila clam (Delgado and Pérez-Camacho, 2007; Laruelle et al., 1994; Moura et al., 2018), may contribute to the observed greater abundance of the introduced clam than of *R. decussatus*, more osmotolerant but with a reproductive strategy based on delayed gonadal development, and also relative to the highly osmosensitive species *C. edule* and *V. corrugata*.

The large, month-dependent variation in the mantle-edge proteome influences the search for potential bivalve salt stress biomarkers. In *V. corrugata* and *C. edule*, more than half of the differentially abundant proteins detected were identified in both months and presented concordant fold changes, constituting potentially useful factors in determining biomarkers of hyposaline stress. In *Ruditapes* spp., however, the small number of differences between salinity treatments and, consequently, the low concordance between months, indicates the low consistency when trying to determine potential biomarkers in these two species. The latter result may be due to both the combination of month-dependent factors that may condition a highly variable stress response between March and May, and that proteins found to be differentially abundant between salinity treatments may not be involved in the response to osmotic stress in *Ruditapes* spp. This was particularly notable in *R. decussatus*, which showed quite small differences between salinity treatments in both months. In *R. philippinarum*, the result could be affected by the reduced detection of proteomic variations in March.

5. Conclusions

Molecular biomarkers of abiotic stress in bivalves have already been described in the presence of contaminants, but recent mass mortality events of clams and cockles due to abrupt reductions in salinity have shifted the focus of the study to hyposaline stress markers.

In this exploratory study, we detected proteins with different relative abundances under hyposaline conditions and concordant fold changes between March and May for the mantle-edge proteome of two highly osmotic stress-sensitive native species, *V. corrugata* and *C. edule*. These proteins, including aquaporin and chaperones, which are involved in detoxification and regulation of ROS rate, lipid membrane remodelling, autophagy and apoptosis, could be useful molecular targets for establishing biomarkers of hyposaline stress response in these bivalve species. In *R. decussatus* and *R. philippinarum*, the small number of differences between salinity treatments detected in this species did not enable the detection of a higher number of proteins with concordant abundances between months than expected by chance. This suggests that the response to saline stress is complex and possibly influenced by other factors in addition to the sampling time. Although these results apply to the mantle-edge proteome, they may vary in other tissues.

To improve the detection of osmotic stress biomarkers considering the information provided in this study about the large molecular variability between months, further investment in transcriptomic and proteomic data in different tissues is needed, especially in *V. corrugata* and *C. edule*, native species of high economic value. Furthermore, if the predictions of increased extreme rainfall are fulfilled, and taking these results into account, the introduced *R. philippinarum* could replace other commercially important species. Determining the key proteins when studying the response to hyposaline conditions would enable the application of faster and more affordable techniques focused on detecting and quantifying target proteins. Tracking the abundance of such proteins, in combination with precipitation monitoring and prediction, could promote the management of optimal collection and commercialisation periods, particularly for native species.

Credit author statement

Sofía Blanco: Conceptualization; Data curation; Formal analysis; Investigation; Methodology; Visualization; Writing – review & editing, **Paloma Morán**: Conceptualization; Data curation; Formal analysis; Investigation; Methodology; Supervision; Visualization; Writing – review & editing, **Ángel Pérez**: Conceptualization; Data curation; Formal analysis; Investigation; Methodology; Supervision; Visualization; Writing – original draft; Writing – review & editing, **Celia Olabarria**: Conceptualization; Funding acquisition; Investigation; Methodology; Writing – review & editing, **Elsa Vázquez**: Conceptualization; Funding acquisition; Investigation; Methodology; Project administration; Supervision; Visualization; Writing – original draft; Writing – review & editing.

Funding

This research was supported by the Spanish Ministerio de Economía y Competitividad (grant CTM2014-51935-R, project MARISCO), the Autonomous government Xunta de Galicia-FEDER (project GRC2013-004 and ED431C 2017/46) and the Xunta de Galicia - Gain project for competitive reference groups (project ED431C 2020/05). Funding for open access charge: Universidade de Vigo/CISUG.

Declaration of competing interest

The authors declare that they have no known competing financial interests or personal relationships that could have appeared to influence the work reported in this paper.

Data availability

The mass spectrometry proteomics data have been deposited to the ProteomeXchange Consortium (Deutsch *et al.*, 2020) via the PRIDE (Perez-Riverol *et al.*, 2019) partner repository with the dataset identifier PXD030926.

Acknowledgements

Facilities were kindly provided by the Estacion de Ciencias Mariñas de Toralla (CIM-ECIMAT) of the Universidade de Vigo. We thank Drs. Sarah Woodin, David Wethey, Laura G. Peteiro, Gonzalo Macho, and Rula Domínguez as well as Esther Pérez, Rula Domínguez, Adriana Álvarez and all the staff at ECIMAT for their support in the laboratory experiments. We also thank J.C. Mariño and L. Solís, technical assistants from the Cofradía de Pescadores of Cambados and Noia respectively, for providing the clams and cockles and valuable comments for the experiments. Finally, we thank Manuel Marcos for carrying out the LC-MS/MS analyses in the CACTI (Universidade de Vigo).

Appendix A. Supplementary data

Supplementary data to this article can be found online at https://doi.org/10.1016/j.envres.2022.114371.

References

Alvarez, I., deCastro, M., Gomez-Gesteira, M., Prego, R., 2005. Inter- and intra-annual analysis of the salinity and temperature evolution in the Galician Rías Baixas–ocean boundary (northwest Spain). J. Geophys. Res.: Oceans 110 (C4). https://doi.org/10.1029/2004JC002504.

Alves de Almeida, E., Celso Dias Bainy, A., Paula de Melo Loureiro, A., Regina Martinez, G., Miyamoto, S., Onuki, J., Fujita Barbosa, L., Carrião Machado Garcia, C., Manso Prado, F., Eliza Ronsein, G., Alexandre Sigolo, C., Barbosa Brochini, C., Maria Gracioso Martins, A., Helena Gennari de Medeiros, M., Di Mascio, P., 2007. Oxidative stress in *Perna perna* and other bivalves as indicators of environmental stress in the Brazilian marine environment: antioxidants, lipid peroxidation and DNA damage. Comp. Biochem. Physiol. Mol. Integr. Physiol. 146 (4), 588–600. https://doi.org/10.1016/j.cbpa.2006.02.040.

Balbi, T., Auguste, M., Ciacci, C., Canesi, L., 2021. Immunological responses of marine bivalves to contaminant exposure: contribution of the -omics approach. Front. Immunol. 12, 618726 https://doi.org/10.3389/fimmu.2021.618726.

Ballantyne, J.S., Moyes, C.D., 1987. Osmotic effects on fatty ccid, pyruvate, and ketone body oxidation in oyster gill mitochondria. Physiol. Zool. 60 (6), 713–721. https://doi.org/10.1086/physzool.60.6.30159987.

Bidegain, G., Juanes, J.A., 2013. Does expansion of the introduced Manila clam Ruditapes philippinarum cause competitive displacement of the European native clam *Ruditapes decussatus*? J. Exp. Mar. Biol. Ecol. 445, 44–52. https://doi.org/10.1016/j.jembe.2013.04.005.

Blum, M., Chang, H.-Y., Chuguransky, S., Grego, T., Kandasaamy, S., Mitchell, A., Nuka, G., Paysan-Lafosse, T., Qureshi, M., Raj, S., Richardson, L., Salazar, G.A., Williams, L., Bork, P., Bridge, A., Gough, J., Haft, D.H., Letunic, I., Marchler-Bauer, A., et al., 2021. The InterPro protein families and domains database: 20 years on. Nucleic Acids Res. 49 (D1), D344–D354. https://doi.org/10.1093/nar/gkaa977.

Brett, J.R., 1979. 10—environmental factors and growth. In: Hoar, En W.S., Randall, D. J., Brett, J.R. (Eds.), Fish Physiology, vol. 8. Academic Press, pp. 599–675. https://doi.org/10.1016/S1546-5098(08)60033-3.

Candas, D., Li, J.J., 2014. MnSOD in oxidative stress response-potential regulation via mitochondrial protein influx. Antioxidants Redox Signal. 20 (10), 1599–1617. https://doi.org/10.1089/ars.2013.5305.

Carregosa, V., Velez, C., Soares, A.M.V.M., Figueira, E., Freitas, R., 2014. Physiological and biochemical responses of three *Veneridae* clams exposed to salinity changes. Comp. Biochem. Physiol. B Biochem. Mol. Biol. 177–178, 1–9. https://doi.org/10.1016/j.cbpb.2014.08.001.

Carvajal-Rodriguez, A., Uña-Alvarez, J. de, 2011. Assessing significance in high-throughput experiments by sequential goodness of fit and q-value estimation. PLoS One 6 (9), e24700. https://doi.org/10.1371/journal.pone.0024700.

Cerviño Otero, A., 2012. Ciclo reproductivo, cultivo en criadero y en el medio natural de la almeja babosa Venerupis pullastra. Montagu, 1803. https://minerva.usc.es/xmlui/handle/10347/3645.

Cianfruglia, L., Morresi, C., Bacchetti, T., Armeni, T., Ferretti, G., 2020. Protection of polyphenols against glyco-oxidative stress: involvement of glyoxalase pathway. Antioxidants 9 (10), 1006. https://doi.org/10.3390/antiox9101006.

Delgado, M., Pérez-Camacho, A., 2005. Histological study of the gonadal development of *Ruditapes decussatus* (L.) (Mollusca: Bivalvia) and its relationship with available food. Sci. Mar. 69, 87–97.

Delgado, M., Pérez-Camacho, A., 2007. Comparative study of gonadal development of *Ruditapes philippinarum* (Adams and Reeve) and *Ruditapes decussatus* (L.) (Mollusca: Bivalvia): influence of temperature. Sci. Mar. 71 (3), 471–484. https://doi.org/10.3989/scimar.2007.71n3471.

Des, M., Fernández-Nóvoa, D., deCastro, M., Gómez-Gesteira, J.L., Sousa, M.C., Gómez-Gesteira, M., 2021. Modeling salinity drop in estuarine areas under extreme precipitation events within a context of climate change: effect on bivalve mortality in Galician Rías Baixas. Sci. Total Environ. 790, 148147 https://doi.org/10.1016/j.scitotenv.2021.148147.

Di Ciano-Oliveira, C., Thirone, A.C.P., Szászi, K., Kapus, A., 2006. Osmotic stress and the cytoskeleton: the R(h)ole of Rho GTPases. Acta Physiol. 187 (1–2), 257–272. https://doi.org/10.1111/j.1748-1716.2006.01535.x.

Diz, A.P., Carvajal-Rodríguez, A., Skibinski, D.O.F., 2011. Multiple hypothesis testing in proteomics: a strategy for experimental work. Mol. Cell. Proteomics: MCP 10 (3). https://doi.org/10.1074/mcp.M110.004374. M110.004374.

Diz, A.P., Sánchez-Marín, P., 2021. A primer and guidelines for shotgun proteomic analysis in non-model organisms. Methods Mol. Biol. 2259, 77–102. https://doi.org/10.1007/978-1-0716-1178-4_6.

Domínguez, R., Vázquez, E., Woodin, S.A., Wethey, D.S., Peteiro, L.G., Macho, G., Olabarria, C., 2020. Sublethal responses of four commercially important bivalves to low salinity. Ecol. Indicat. 111, 106031 https://doi.org/10.1016/j.ecolind.2019.106031.

Eymann, C., Götze, S., Bock, C., Guderley, H., Knoll, A.H., Lannig, G., Sokolova, I.M., Aberhan, M., Pörtner, H.-O., 2020. Thermal performance of the European flat oyster, *Ostrea edulis* (Linnaeus, 1758)—explaining ecological findings under climate change. Mar. Biol. 167 (2), 17. https://doi.org/10.1007/s00227-019-3620-3.

Field, C.B., Behrenfeld, M.J., Randerson, J.T., Falkowski, P., 1998. Primary production of the biosphere: integrating terrestrial and oceanic components. Science 281 (5374), 237–240. https://doi.org/10.1126/science.281.5374.237.

Gharbi, A., Farcy, E., Van Wormhoudt, A., Denis, F., 2016. Response of the carpet shell clam (*Ruditapes decussatus*) and the Manila clam (*Ruditapes philippinarum*) to salinity stress. Biologia 71 (5), 551–562. https://doi.org/10.1515/biolog-2016-0072.

Grilo, T.F., Cardoso, P.G., Dolbeth, M., Bordalo, M.D., Pardal, M.A., 2011. Effects of extreme climate events on the macrobenthic communities' structure and functioning of a temperate estuary. Mar. Pollut. Bull. 62 (2), 303–311. https://doi.org/10.1016/j.marpolbul.2010.10.010.

Harley, C.D.G., Randall Hughes, A., Hultgren, K.M., Miner, B.G., Sorte, C.J.B., Thornber, C.S., Rodriguez, L.F., Tomanek, L., Williams, S.L., 2006. The impacts of climate change in coastal marine systems. Ecol. Lett. 9 (2), 228–241. https://doi.org/10.1111/j.1461-0248.2005.00871.x.

Hauton, C., 2016. Effects of Salinity as a Stressor to Aquatic Invertebrates, pp. 3–24. https://doi.org/10.1093/acprof:oso/9780198718826.003.0001.

Holland, D., 1974. Reproductive cycle of the Manila clam (*Venerupis japonica*), from food canal, Washington. Proc. Natl. Shellfish. Assoc. 64, 53–58.

Holt, C., Yandell, M., 2011. MAKER2: an annotation pipeline and genome-database management tool for second-generation genome projects. BMC Bioinf. 12 (1), 491. https://doi.org/10.1186/1471-2105-12-491.

Ito, T., Yamazaki, M., 2006. The "Le Chatelier's principle"-Governed response of actin filaments to osmotic stress. J. Phys. Chem. B 110 (27), 13572–13581. https://doi.org/10.1021/jp060612r.

Joaquim, S., Matias, D., Matias, A.M., Moura, P., Arnold, W.S., Chícharo, L., Gaspar, M. B., 2011. Reproductive activity and biochemical composition of the pullet carpet shell *Venerupis senegalensis* (Gmelin, 1791) (Mollusca: Bivalvia) from Ria de Aveiro (northwestern coast of Portugal). Sci. Mar. 75 (2), 217–226. https://doi.org/10.3989/scimar.2011.75n2217.

Johnson, G.L., Nakamura, K., 2007. The c-Jun kinase/stress-activated pathway: regulation, function and role in human disease. Biochim. Biophys. Acta 1773 (8), 1341–1348. https://doi.org/10.1016/j.bbamcr.2006.12.009.

Juanes, J.A., Bidegain, G., Echavarri-Erasun, B., Puente, A., García, A., García, A., Bárcena, J.F., Álvarez, C., García-Castillo, G., 2012. Differential distribution pattern of native Ruditapes decussatus and introduced *Ruditapes phillippinarum* clam populations in the Bay of Santander (Gulf of Biscay): considerations for fisheries management. Ocean Coast Manag. 69, 316–326. https://doi.org/10.1016/j.ocecoaman.2012.08.007.

Kilfoil, P.J., Tipparaju, S.M., Barski, O.A., Bhatnagar, A., 2013. Regulation of ion channels by pyridine nucleotides. Circ. Res. 112 (4), 721–741. https://doi.org/10.1161/CIRCRESAHA.111.247940.

Kino, T., Segars, J.H., Chrousos, G.P., 2010. The guanine nucleotide exchange factor Brx: a link between osmotic stress, inflammation and organ physiology and pathophysiology. Expet Rev. Endocrinol. Metabol. 5 (4), 603–614. https://doi.org/10.1586/eem.10.3.

Kooijman, B., Kooijman, S.A.L.M., 2010. Dynamic Energy Budget Theory for Metabolic Organisation. Cambridge University Press.

Laruelle, F., Guillou, J., Paulet, Y.M., 1994. Reproductive pattern of the clams, *Ruditapes decussatus* and *R. philippinarum* on intertidal flats in Brittany. J. Mar. Biol. Assoc. U. K. 74 (2), 351–366. https://doi.org/10.1017/S0025315400039382.

Lei, Y., Wen, H., Yu, Y., Taxman, D.J., Zhang, L., Widman, D.G., Swanson, K.V., Wen, K.-W., Damania, B., Moore, C.B., Giguère, P.M., Siderovski, D.P., Hiscott, J., Razani, B., Semenkovich, C.F., Chen, X., Ting, J.P.-Y., 2012. The mitochondrial proteins NLRX1 and TUFM form a complex that regulates type I interferon and autophagy. Immunity 36 (6), 933–946. https://doi.org/10.1016/j.immuni.2012.03.025.

Li, M., Liu, Y., Xia, F., Wu, Z., Deng, L., Jiang, R., Guo, F.-J., 2014. Progranulin is required for proper ER stress response and inhibits ER stress-mediated apoptosis through TNFR2. Cell. Signal. 26 (7), 1539–1548. https://doi.org/10.1016/j.cellsig.2014.03.026.

Lin, C.-H., Yeh, P.-L., Lee, T.-H., 2016. Ionic and amino acid regulation in hard clam (*Meretrix lusoria*) in Response to Salinity Challenges. Front. Physiol. 7. https://www.frontiersin.org/article/10.3389/fphys.2016.00368.

Lu, Y., Parker, K. h, Wang, W., 2006. Effects of osmotic pressure in the extracellular matrix on tissue deformation. Phil. Trans. Math. Phys. Eng. Sci. 364 (1843), 1407–1422. https://doi.org/10.1098/rsta.2006.1778.

Martínez-Castro, C., Vázquez, E., 2012. Reproductive cycle of the cockle *Cerastoderma edule* (linnaeus 1758) in the ría de Vigo (Galicia, northwest Spain). J. Shellfish Res. 31 (3), 757–767. https://doi.org/10.2983/035.031.0320.

Massudi, H., Grant, R., Guillemin, G.J., Braidy, N., 2012. NAD^+ metabolism and oxidative stress: the golden nucleotide on a crown of thorns. Redox Rep. 17 (1), 28–46. https://doi.org/10.1179/1351000212Y.0000000001.

Mateos, J., Estévez, O., González-Fernández, Á., Anibarro, L., Pallarés, Á., Reljic, R., Gallardo, J.M., Medina, I., Carrera, M., 2019. High-resolution quantitative proteomics applied to the study of the specific protein signature in the sputum and saliva of active tuberculosis patients and their infected and uninfected contacts. J. Proteonomics 195, 41–52. https://doi.org/10.1016/j.jprot.2019.01.010.

Méndez, G., Vilas, F., 2005. Geological antecedents of the Rias Baixas (Galicia, northwest iberian peninsula). J. Mar. Syst. 54 (1), 195–207. https://doi.org/10.1016/j.jmarsys.2004.07.012.

Meng, J., Zhu, Q., Zhang, L., Li, C., Li, L., She, Z., Huang, B., Zhang, G., 2013. Genome and transcriptome analyses provide insight into the euryhaline adaptation mechanism of *Crassostrea gigas*. PLoS One 8 (3), e58563. https://doi.org/10.1371/journal.pone.0058563.

Metsalu, T., Vilo, J., 2015. ClustVis: a web tool for visualizing clustering of multivariate data using Principal Component Analysis and heatmap. Nucleic Acids Res. 43 (W1), W566–W570. https://doi.org/10.1093/nar/gkv468.

Moura, P., Vasconcelos, P., Pereira, F., Chainho, P., Costa, J.L., Gaspar, M.B., 2018. Reproductive cycle of the Manila clam (*Ruditapes philippinarum*): an intensively harvested invasive species in the Tagus Estuary (Portugal). J. Mar. Biol. Assoc. U. K. 98 (7), 1645–1657. https://doi.org/10.1017/S0025315417001382.

Muraeva, O., Maltseva, A., Varfolomeeva, M., Mikhailova, N., Granovitch, A., 2017. Mild osmotic stress in intertidal gastropods *Littorina saxatilis* and *L. obtusata* (Mollusca: caenogastropoda): a proteomic analysis. Biol. Commun. 62, 202–213. https://doi.org/10.21638/11701/spbu03.2017.305.

Osmanagic-Myers, S., Rus, S., Wolfram, M., Brunner, D., Goldmann, W.H., Bonakdar, N., Fischer, I., Reipert, S., Zuzuarregui, A., Walko, G., Wiche, G., 2015. Plectin reinforces vascular integrity by mediating crosstalk between the vimentin and the actin networks. J. Cell Sci. 128 (22), 4138–4150. https://doi.org/10.1242/jcs.172056.

País, S.M., Téllez-Iñón, M.T., Capiati, D.A., 2009. Serine/threonine protein phosphatases type 2A and their roles in stress signaling. Plant Signal. Behav. 4 (11), 1013–1015.

Parada, J.M., Molares, J., 2008. Natural mortality of the cockle *Cerastoderma edule* (L.) from the Ria of Arousa (NW Spain) intertidal zone. Rev. Biol. Mar. Oceanogr. 43 (3), 501–511. https://doi.org/10.4067/S0718-19572008000300009.

Parada, J.M., Molares, J., Otero, X., 2012. Multispecies mortality patterns of commercial bivalves in relation to estuarine salinity fluctuation. Estuar. Coast 35 (1), 132–142. https://doi.org/10.1007/s12237-011-9426-2.

Peteiro, L.G., Woodin, S.A., Wethey, D.S., Costas-Costas, D., Martínez-Casal, A., Olabarria, C., Vázquez, E., 2018. Responses to salinity stress in bivalves: evidence of ontogenetic changes in energetic physiology on *Cerastoderma edule*. Sci. Rep. 8 (1), 8329. https://doi.org/10.1038/s41598-018-26706-9.

Petes, L.E., Menge, B.A., Harris, A.L., 2008. Intertidal mussels exhibit energetic trade-offs between reproduction and stress resistance. Ecol. Monogr. 78 (3), 387–402. https://doi.org/10.1890/07-0605.1.

Pörtner, H.O., Farrell, A.P., 2008. Physiology and climate change. Science 322 (5902), 690–692. https://doi.org/10.1126/science.1163156.

Pourmozaffar, S., Tamadoni Jahromi, S., Rameshi, H., Sadeghi, A., Bagheri, T., Behzadi, S., Gozari, M., Zahedi, M.R., Abrari Lazarjani, S., 2020. The role of salinity in physiological responses of bivalves. Rev. Aquacult. 12 (3), 1548–1566. https://doi.org/10.1111/raq.12397.

Rambold, A.S., Lippincott-Schwartz, J., 2011. Mechanisms of mitochondria and autophagy crosstalk. Cell Cycle 10 (23), 4032–4038. https://doi.org/10.4161/cc.10.23.18384.

Redza-Dutordoir, M., Averill-Bates, D.A., 2016. Activation of apoptosis signalling pathways by reactive oxygen species. Biochim. Biophys. Acta Mol. Cell Res. 1863 (12), 2977–2992. https://doi.org/10.1016/j.bbamcr.2016.09.012.

Saito, M., Iestamantavicius, V., Hess, D., Matthias, P., 2021. Monitoring acetylation of the RNA helicase DDX3X, a protein critical for formation of stress granules. In: Boudvillain, En M. (Ed.), RNA Remodeling Proteins: Methods and Protocols. Springer US, pp. 217–234. https://doi.org/10.1007/978-1-0716-0935-4_14.

Sánchez-Marín, P., Vidal-Liñán, L., Fernández-González, L.E., Montes, R., Rodil, R., Quintana, J.B., Carrera, M., Mateos, J., Diz, A.P., Beiras, R., 2021. Proteomic analysis and biochemical alterations in marine mussel gills after exposure to the organophosphate flame retardant TDCPP. Aquat. Toxicol. 230, 105688 https://doi.org/10.1016/j.aquatox.2020.105688.

Shim, E.-H., Kim, J.-I., Bang, E.-S., Heo, J.-S., Lee, J.-S., Kim, E.-Y., Lee, J.-E., Park, W.-Y., Kim, S.-H., Kim, H.-S., Smithies, O., Jang, J.-J., Jin, D.-I., Seo, J.-S., 2002. Targeted disruption of hsp70.1 sensitizes to osmotic stress. EMBO Rep. 3 (9), 857–861. https://doi.org/10.1093/embo-reports/kvf175.

Soares Moretti, A.I., Martins Laurindo, F.R., 2017. Protein disulfide isomerases: redox connections in and out of the endoplasmic reticulum. Arch. Biochem. Biophys. 617, 106–119. https://doi.org/10.1016/j.abb.2016.11.007.

Steffen, J.B.M., Falfushynska, H.I., Piontkivska, H., Sokolova, I.M., 2020. Molecular biomarkers of the mitochondrial quality control are differently affected by hypoxia-reoxygenation stress in marine bivalves *Crassostrea gigas* and *Mytilus edulis*. Front. Mar. Sci. 7. https://www.frontiersin.org/article/10.3389/fmars.2020.604411.

Stewart, G.W., 1997. Stomatin. Int. J. Biochem. Cell Biol. 29 (2), 271–274. https://doi.org/10.1016/S1357-2725(96)00072-6.

Storz, P., 2011. Forkhead Homeobox Type O transcription factors in the responses to oxidative stress. Antioxidants Redox Signal. 14 (4), 593. https://doi.org/10.1089/ars.2010.3405.

Stumpp, M., Trübenbach, K., Brennecke, D., Hu, M.Y., Melzner, F., 2012. Resource allocation and extracellular acid–base status in the sea urchin *Strongylocentrotus droebachiensis* in response to CO_2 induced seawater acidification. Aquat. Toxicol. 110–111, 194–207. https://doi.org/10.1016/j.aquatox.2011.12.020.

Sydow, K., Daiber, A., Oelze, M., Chen, Z., August, M., Wendt, M., Ullrich, V., Mülsch, A., Schulz, E., Keaney, J.F., Stamler, J.S., Münzel, T., 2004. Central role of mitochondrial aldehyde dehydrogenase and reactive oxygen species in nitroglycerin tolerance and cross-tolerance. J. Clin. Investig. 113 (3), 482–489. https://doi.org/10.1172/JCI19267.

Tang, B., Wang, S., Wang, S.-G., Wang, H.-J., Zhang, J.-Y., Cui, S.-Y., 2018. Invertebrate trehalose-6-phosphate synthase gene: genetic architecture, biochemistry, physiological function, and potential applications. Front. Physiol. 9. https://www.frontiersin.org/article/10.3389/fphys.2018.00030.

Team, Rs, 2020. RStudio: Integrated Development for R. RStudio, PBC, Boston. MA. http://www.rstudio.com.

Timmins-Schiffman, E.B., Crandall, G.A., Vadopalas, B., Riffle, M.E., Nunn, B.L., Roberts, S.B., 2017. Integrating discovery-driven proteomics and selected reaction monitoring to develop a noninvasive assay for geoduck reproductive maturation. J. Proteome Res. 16 (9), 3298–3309. https://doi.org/10.1021/acs.jproteome.7b00288.

Tomanek, L., 2012. Environmental proteomics of the mussel *Mytilus*: implications for tolerance to stress and change in limits of biogeographic ranges in response to climate change. Integr. Comp. Biol. 52 (5), 648–664. https://doi.org/10.1093/icb/ics114.

Tomanek, L., Zuzow, M.J., Hitt, L., Serafini, L., Valenzuela, J.J., 2012. Proteomics of hyposaline stress in blue mussel congeners (genus *Mytilu*): implications for biogeographic range limits in response to climate change. J. Exp. Biol., 076448 https://doi.org/10.1242/jeb.076448 jeb.

Van Houtven, J., Hooyberghs, J., Laukens, K., Valkenborg, D., 2021. CONSTANd: an efficient normalization method for relative quantification in small- and large-scale omics experiments in R BioConductor and Python. J. Proteome Res. 20 (4), 2151–2156. https://doi.org/10.1021/acs.jproteome.0c00977.

Vázquez, E., Woodin, S.A., Wethey, D.S., Peteiro, L.G., Olabarria, C., 2021. Reproduction under stress: acute effect of low salinities and heat waves on reproductive cycle of four ecologically and commercially important bivalves. Front. Mar. Sci. 8. https://www.frontiersin.org/article/10.3389/fmars.2021.685282.

Verdelhos, T., Marques, J.C., Anastácio, P., 2015. The impact of estuarine salinity changes on the bivalves *Scrobicularia plana* and *Cerastoderma edule*, illustrated by behavioral and mortality responses on a laboratory assay. Ecol. Indicat. 52, 96–104. https://doi.org/10.1016/j.ecolind.2014.11.022.

Viceto, C., Cardoso Pereira, S., Rocha, A., 2019. Climate change projections of extreme temperatures for the Iberian Peninsula. Atmosphere 10 (5), 229. https://doi.org/10.3390/atmos10050229.

Vinogradov, A.D., Grivennikova, V.G., 2016. Oxidation of NADH and ROS production by respiratory complex I. Biochim. Biophys. Acta Bioenerg. 1857 (7), 863–871. https://doi.org/10.1016/j.bbabio.2015.11.004.

Wang, Y., Branicky, R., Noë, A., Hekimi, S., 2018. Superoxide dismutases: dual roles in controlling ROS damage and regulating ROS signaling. J. Cell Biol. 217 (6), 1915–1928. https://doi.org/10.1083/jcb.201708007.

Woodin, S.A., Wethey, D.S., Olabarria, C., Vázquez, E., Domínguez, R., Macho, G., Peteiro, L., 2020. Behavioral responses of three venerid bivalves to fluctuating salinity stress. J. Exp. Mar. Biol. Ecol. 522, 151256 https://doi.org/10.1016/j.jembe.2019.151256.

Zhao, X., Yu, H., Kong, L., Li, Q., 2012. Transcriptomic responses to salinity stress in the pacific oyster *Crassostrea gigas*. PLoS One 7 (9), e46244. https://doi.org/10.1371/journal.pone.0046244.

Further reading

Perez-Riverol, Y., Csordas, A., Bai, J., Bernal-Llinares, M., Hewapathirana, S., Kundu, D. J., et al., 2019. The PRIDE database and related tools and resources in 2019: improving support for quantification data. Nucleic Acids Res 47, D442–D450. https://doi.org/10.1093/nar/gky1106.

Deutsch, E.W., Bandeira, N., Sharma, V., Perez-Riverol, Y., Carver, J.J., Kundu, D.J., et al., 2020. The ProteomeXchange consortium in 2020: enabling "big data" approaches in proteomics. Nucleic Acids Res 48, D1145–D1152. https://doi.org/10.1093/nar/gkz984.